Journal of Materials Science and Chemical Engineering, 2025, 13(6), 1-9
https://www.scirp.org/journal/msce
ISSN Online: 2327-6053
ISSN Print: 2327-6045

Thermoelectric Effect of $Ca_2Fe_2O_5$ at Low Temperatures

Ebony Schultz, Ram Krishna Hona*

Environmental Science Department, United Tribes Technical College, Bismarck, ND, USA
Email: *rhona@uttc.edu

How to cite this paper: Schultz, E. and Hona, R.K. (2025) Thermoelectric Effect of Ca2Fe2O5 at Low Temperatures. *Journal of Materials Science and Chemical Engineering*, **13**, 1-9.
https://doi.org/10.4236/msce.2025.136001

Received: April 26, 2025
Accepted: June 8, 2025
Published: June 11, 2025

Copyright © 2025 by author(s) and Scientific Research Publishing Inc.
This work is licensed under the Creative Commons Attribution International License (CC BY 4.0).
http://creativecommons.org/licenses/by/4.0/
Open Access

Abstract

This study investigates the thermoelectric properties of $Ca_2Fe_2O_5$ over a temperature range of 7˚C to 50˚C. The experiment measured the voltage generated by temperature differences across two sides of the material, with a focus on the voltage response at temperatures both below and above room temperature. Results indicate that at lower temperatures (7˚C to 15˚C), the voltage generated by the temperature difference was higher, though not directly proportional to the magnitude of the temperature gradient. The highest voltage recorded for the smallest temperature difference in this range was 109 mV, observed between 14.6˚C and 17.6˚C (smallest temperature difference, 3˚C). Similarly, at temperatures above room temperature, the voltage generated was relatively lower, peaking at 125 mV between 9˚C and 44˚C (higher temperature difference). These results suggest complex behavior of $Ca_2Fe_2O_5$'s thermoelectric response, with non-linear relationships between voltage and temperature differences at both low and high temperatures.

Keywords

XRD, Solid-State Reaction, Perovskite Oxides, Oxygen Deficiency, Thermoelectric

1. Introduction

Thermoelectric materials, which can convert temperature gradients into electrical energy through the Seebeck effect, have emerged as promising candidates for renewable energy generation and efficient thermal management systems. These materials are pivotal in applications such as waste heat recovery [1], thermoelectric generators (TEGs), [2] and Peltier coolers [3], where direct thermal-to-electrical energy conversion plays a crucial role. The performance of thermoelectric materials is typically characterized by their Seebeck coefficient (S), electrical conduc-

tivity (σ), and thermal conductivity (κ), which collectively define the dimensionless figure of merit (ZT). A high ZT value indicates a material with efficient thermoelectric performance, and researchers have focused on discovering and optimizing materials with large Seebeck coefficients, low thermal conductivity, and favorable electrical conductivity to achieve higher ZT values. Common materials such as bismuth telluride (Bi_2Te_3) and lead telluride (PbTe) have demonstrated high ZT values, particularly at room temperature, but issues such as scarcity, toxicity, and high cost have driven the search for alternative, more sustainable materials.

Perovskite oxides, in particular, have attracted attention due to their structural flexibility and tunable electronic properties. These materials, with the general formula ABO_3, offer the possibility of tailoring their thermoelectric properties through chemical substitution, crystal engineering, and defect management. Among these, $Ca_2Fe_2O_5$, a brownmillerite phase of calcium ferrite, is of interest because of its mixed valence states and potential for exhibiting interesting electrical and thermal properties [4] [5]. Previous studies have explored the electrical and ionic conductivity of perovskite and brownmillerite-type materials, highlighting their complex conduction mechanisms and sensitivity to oxygen vacancy concentrations. However, there is limited literature on the thermoelectric behavior of $Ca_2Fe_2O_5$ particularly its performance across a broad range of temperatures [6].

Complex oxides, including perovskites, have been noted for their stability at high temperatures, making them attractive candidates for high-temperature thermoelectric applications [7]. Studies on related materials, such as $CaMnO_3$ and $SrTiO_3$ have demonstrated non-linear voltage responses to temperature gradients, particularly at temperatures both above and below room temperature [8]. The Seebeck coefficient is a critical parameter in thermoelectrics, as it measures the voltage generated per unit temperature gradient across a material. For materials with low thermoelectric figure of merit (ZT), the Seebeck coefficient often plays a limiting role. A low Seebeck coefficient reduces the material's ability to convert thermal energy into electrical energy effectively, hindering performance. Improving the Seebeck coefficient, typically by optimizing the carrier concentration or material composition, is essential for enhancing ZT and advancing thermoelectric applications in energy harvesting and waste heat recovery. Note that the Seebeck coefficient describes the material's efficiency in converting temperature gradients into electrical voltage. A positive Seebeck coefficient indicates that positive charge carriers (holes) dominate the thermoelectric response, while a negative coefficient suggests the dominance of negative charge carriers (electrons).

Seebeck coefficient (S) = voltage/temperature difference

The Seebeck coefficient (S) is a measure of the thermoelectric voltage generated in response to a temperature difference across a material. It is mathematically expressed as:

$$S = \Delta V / \Delta T$$

Where:

- S is the Seebeck coefficient (typically in volts per kelvin, V/K or microvolts per kelvin, μV/K),
- ΔV is the voltage difference (V) between the two ends of the material,
- ΔT is the temperature difference (K) between the two sides of the material.

In this study, we investigate the thermoelectric properties of $Ca_2Fe_2O_5$ across a temperature range from 7˚C to 55˚C, with a particular focus on its behavior in regimes both below and above room temperature. The material's response to temperature gradients is analyzed to determine how the Seebeck coefficient and voltage output vary across this temperature range. This research aims to expand the understanding of $Ca_2Fe_2O_5$'s thermoelectric performance and its potential applications in temperature-sensing and energy-harvesting technologies.

2. Experimental Method

2.1. Material Synthesis

$Ca_2Fe_2O_5$ was synthesized using a solid-state reaction method. Stoichiometric amounts of high purity starting materials, including calcium carbonate ($CaCO_3$) and iron (III) oxide (Fe_2O_3) and manganese oxide (MnO_2), were carefully weighed and thoroughly mixed. The mixtures were ground using an agate mortar and pestle to achieve homogeneous powders.

The resulting powders were pressed into pellets and subjected to a two-step thermal treatment. Initially, the samples were calcined at 1000˚C for 24 hours in MTI muffle furnace, with a ramping rate of 100˚C per hour to ensure controlled heating. After cooling, the pellets were reground, pressed again into pellets, and heated at 1200˚C for an additional 24 hours under the same ramping rate. Following the final heat treatment, the pellets were allowed to cool to room temperature naturally inside the furnace.

2.2. Characterization

The phase purity of the synthesized compounds was confirmed using Bruker D2 phaser X-ray diffractometer (XRD) with Cu Kα1 (λ = 1.54056 Å). Rietveld refinements were conducted using GSAS software and the EXPEGUI interface. The microstructures were studied using high resolution field emission scanning electron microscopy (JEOL-SEM).

2.3. Thermoelectric Effect Measurement

The thermoelectric effect was measured by measuring the potential developed by the temperature difference between the two sides of the pellet. A custom designed set up instrument was used to measure it. It contains hollow tubes connected to a hollow cube on two opposite sides for water outlet and inlet. Ice-cold water was run to a metal cubic hollow box through the tube. It keeps the box wall cold all the time. A sample pellet was kept intact with the metal box wall. The temperature of the box wall in contact with the pellet was measured with a k-type thermometer. At the same time the other side (outside) of the pellet was heated with a metal

sheet. The metal sheet was heated by an electric heater such as high temperature soldering heater with controller. The temperature of the outside (heated part) of the pellet was measured by another K-type thermometer. Similarly, the potential difference developed by the hot and cold sides was measured using a voltmeter. Thus, the temperature difference between the two sides of a pellet and the potential (voltage) developed were measured at the same time. The whole set-up was diagrammatically shown in Figure 1.

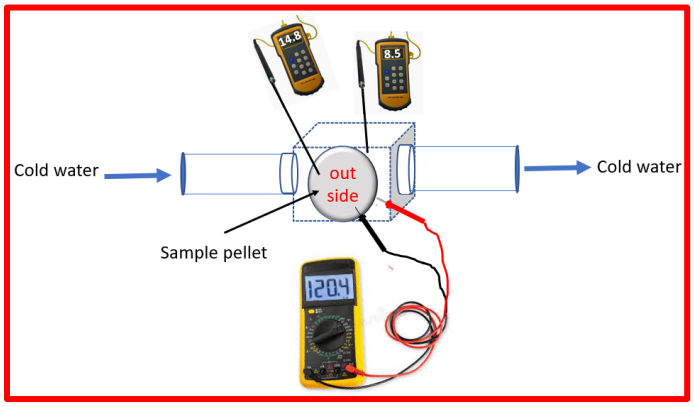

Figure 1. Schematic picture of potential measurement between hot and cold sides of a $Ca_2Fe_2O_5$ pellet.

3. Results and Discussions

3.1. Material Synthesis and Characterization

$Ca_2Fe_2O_5$ was synthesized using the solid-state synthesis technique. The crystal structure of $Ca_2Fe_2O_5$ has been previously reported. [4] To further investigate its structural properties, powder X-ray diffraction (XRD), and scanning electron microscopy (SEM) were employed.

Figure 2 presents the powder XRD data for $Ca_2Fe_2O_5$, confirming its crystal structure through Rietveld refinement. The refinement results were consistent with the previously reported brownmillerite structure characterized by the *Pnma* space group. The refinement also highlighted the alternating arrangement of tetrahedra and octahedra within orthorhombic unit cells. In this structure, tetrahedra within the same layer are aligned in the same direction, while tetrahedra in alternating layers are oriented oppositely. This is visually depicted in Figure 2 inset, where Blue tetrahedra indicates a rightward orientation, and red tetrahedra indicates a leftward orientation. The refined structural parameters of $Ca_2Fe_2O_5$ are provided in Table 1.

Table 1. Rietveld refinement parameters of $Ca_2Fe_2O_{6-\delta}$.

element	x	y	z	Uiso	multiplicity	occupancy
Ca	0.4808(5)	0.1079(2)	0.0247(6)	0.028	8	1
Fe1	0.0000	0.0000	0.0000	0.027(6)	4	1
Fe2	−0.0548(3)	0.2500	−0.0669(9)	0.030(2)	4	1

Continued

O1	0.2573(2)	−0.0154	0.2344(2)	0.027(3)	8	1
O2	0.0295(2)	0.1420(3)	0.0774(2)	0.019(1)	8	1
O3	0.6106(7)	0.2500	−0.1250(5)	0.014(2)	4	1

Space group = *Pnma*, a = 5.4024(1) Å, b = 14.7017(3) Å, c = 5.5726(3) Å, wRp =0.0177, Rp = 0.0132.

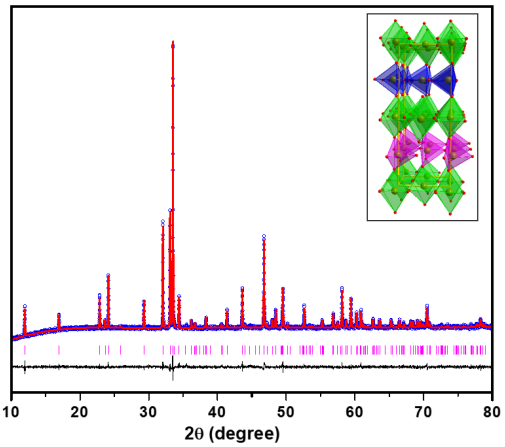

Figure 2. The Rietveld refinement profile of $Ca_2Fe_2O_{6-\delta}$. The blue circles, red line, pink vertical lines, and black solid line represent the raw data, the model, Bragg peak positions, and difference plot, respectively. The inset shows the crystal structure with an orthorhombic unit cell and *Pnma* space group.

The scanning electron microscopy (SEM) image of $Ca_2Fe_2O_5$, shown in **Figure 3**, reveals close contact between the grains. The SEM analysis indicates that the material is non-porous. The non-porosity was evaluated using a theoretical density calculation based on the method described in the literature [6]. The experimental density of $Ca_2Fe_2O_5$ was found to be 98% of the theoretical value, further corroborating the non-porous nature of the bulk material. Despite variations in grain size, larger grains were observed to dominate over smaller ones, as depicted in the SEM image.

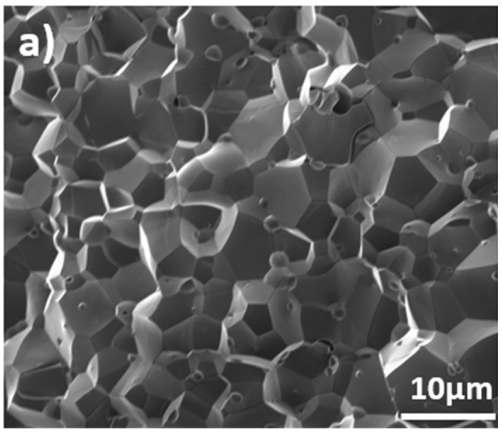

Figure 3. SEM images of $Ca_2Fe_2O_5$.

3.2. Thermoelectric effect

The thermoelectric behavior of $Ca_2Fe_2O_5$ was investigated across a range of temperatures from 7.5˚C to 50˚C. The results, summarized in Table 2, show the voltage "generated by temperature differences (ΔT) and the corresponding thermoelectric effect," S = V/ΔT, where V is the measured voltage in millivolts (mV) and ΔT is the temperature difference in Celsius. Seebeck coefficient S indicates the material's efficiency in converting thermal gradients into electrical voltage.

3.2.1. Voltage Response with Temperature Difference

At lower temperatures (7.5˚C to 17.6˚C), the voltage generated increased with the temperature difference, although this relationship was not linear. For instance, the highest voltage (109 mV) was observed with a small temperature difference of 3˚C between 14.6˚C and 17.6˚C. This suggests that even small temperature gradients can lead to significant voltage generation under certain conditions. As the temperature difference increased in this range (e.g., from 6˚C to 6.3˚C between 7.5˚C and 13.5˚C), the voltage also increased, with a peak value of 120 mV at a difference of 6.3˚C.

However, at higher temperatures (above room temperature), the voltage response began to exhibit more variability. For example, between 30˚C and 47˚C, the voltage generated ranged from 55 mV at a temperature difference of 17˚C to 45 mV at a difference of 25˚C. This suggests that the material's efficiency in generating voltage diminishes as the temperature rises, possibly due to a reduction in the material's thermoelectric potential at higher temperatures.

3.2.2. Seebeck Coefficient (S)

The Seebeck effect refers to the generation of an electromotive force (emf) across two points of an electrically conductive material when there is a temperature gradient between them. This emf is known as the Seebeck emf, or thermoelectric emf. The Seebeck coefficient is the ratio of the emf to the temperature difference. A thermocouple measures the potential difference between the hot and cold ends of two dissimilar materials, and this potential difference is proportional to the temperature difference between the two ends. The value of S shows a decreasing trend with increasing temperature differences. At lower temperatures, for example, when the temperature difference was 3˚C (between 14.6˚C and 17.6˚C), the thermoelectric figure of merit was notably high (36.33), indicating efficient voltage generation with a relatively small temperature gradient. In contrast, at higher temperatures with larger temperature differences, S values were considerably lower. For instance, between 30˚C and 55˚C, the S values decreased significantly, with the lowest value (1.8) recorded for a temperature difference of 25˚C. Table 2 shows the relation between the temperature gradient and Seebeck coefficient. Figure 4 shows the relation between the Seebeck coefficient and the lowest (cold) temperatures at which voltages were measured. Table 3 compares the Seebeck coefficient values with other reported materials.

This trend suggests that while the material is capable of generating relatively high voltage at small temperature differences, its efficiency decreases as the tem-

perature gradient increases. Such behavior may be indicative of the material's non-linear thermoelectric response, possibly due to intrinsic properties like electron scattering, phonon-electron interactions, or thermal conductivity changes at higher temperatures.

Table 2. Temperature gradient, voltage generated and calculated Seebeck coefficient.

Temperature-1 (˚C)	Temperature-2 (˚C)	Difference in temperature	Voltage (mV)	$S = \frac{V}{\Delta T}$ (mV/˚C)
7.5	13.5	6	90 m V	15
8.5	14.8	6.3	120 mV	19.04762
14.6	17.6	3	109 mV	36.33333
13.8	17.6	3.8	103 mV	27.10526
25	30	5	72 mV	14.4
30	38.5	8.5	85 mV	10
26	38	12	34 mV	2.833333
28	40	12	40 mV	3.333333
28	42	14	50 mV	3.571429
30	47	17	55 mV	3.235294
30	55	25	45 mV	1.8
8	26	18	80	4.444444
9	30	21	110	5.238095
9	44	35	125	3.571429
10	50	40	125	3.125

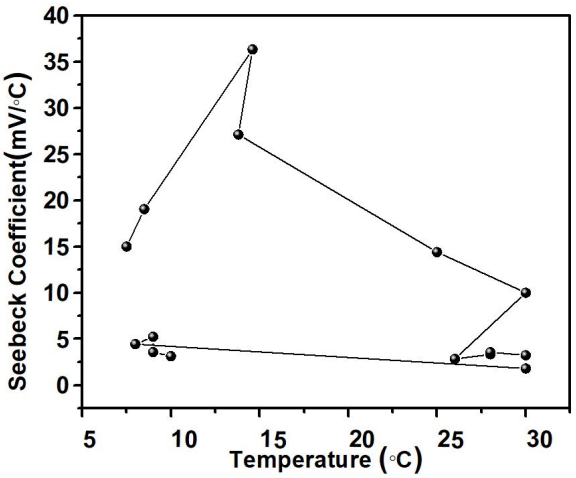

Figure 4. Seebeck coefficient vs temperature (˚C).

Table 3. Comparison of Seebeck coefficients.

compound	Seebeck coefficient (μV/K)	Temperature	References
$Ca_2Fe_2O_5$	- 400	(at 300 K)	doi: 10.1016/j.jssc.2010.05.016 [6]
$LaCoO_3$	- 600	(at 300 K)	https://doi.org/10.1016/j.ceramint.2014.04.123 [9]
$NaCo_2O_4$	- 100	(300 - 1000 K)	DOI: https://doi.org/10.1103/PhysRevB.56.R12685 [10]
$CaMnO_3$	- 550	(at 300 K)	https://doi.org/10.1039/C4TA01514B [11] DOI: 10.1088/1674-1056/24/9/098101 [12]

3.2.3. Interpretation of Trends

The high voltage at smaller temperature differences and the decrease in S at larger gradients can be attributed to several factors:

1) Non-linear thermoelectric response: The material exhibits a complex thermoelectric behavior, where smaller temperature differences result in a more efficient conversion of thermal gradients into voltage. However, as the temperature difference increases, the voltage generated no longer increases proportionally.

2) Material-specific properties: $Ca_2Fe_2O_5$ may exhibit a saturation effect in its thermoelectric response at higher temperatures, where the voltage generated reaches a plateau or decreases slightly with further increases in temperature difference. This suggests that the material's thermoelectric properties are sensitive to both the magnitude and direction of temperature gradients.

3) Thermal conductivity and Seebeck coefficient: The decrease in S at higher temperature differences could also be due to an increase in thermal conductivity, which could reduce the effective temperature gradient across the material, thus lowering its voltage output.

4. Conclusion

The results highlight the intricate thermoelectric behavior of $Ca_2Fe_2O_5$, showing that the material exhibits relatively high voltage generation at small temperature differences, particularly in the lower temperature range (7.5˚C to 17.6˚C). However, as the temperature difference increases, the material's thermoelectric efficiency decreases, reflected in lower S values at higher temperature gradients. These findings suggest that $Ca_2Fe_2O_5$ could be a promising material for thermoelectric applications in specific temperature ranges, particularly where small temperature gradients are involved. Further studies could focus on optimizing the material's performance at higher temperatures and exploring the underlying mechanisms responsible for its non-linear response.

Acknowledgements

This work is partly supported by the National Science Foundation Tribal College and University Program Instructional Capacity Excellence in TCUP Institutions (ICE-TI) grant award # 2225648. A part of this work is supported by NSF TCUP Tribal Enterprise Advancement Center Grant No. HRD 1839895. A part of the work is supported by AIHEC-coordinated NASA TCU Building Bridges, Grant Number 80NSSC24M0025. Additional support for the work came from ND EPSCOR STEM equipment grants. Permission was granted by the United Tribes Technical Colleges (UTTC) Environmental Science Department to publish this information. The views expressed are those of the authors and do not necessarily represent those of United Tribes Technical College.

Conflicts of Interest

The authors declare no conflicts of interest regarding the publication of this paper.

References

[1] Singh, R., Dogra, S., Dixit, S., Vatin, N.I., Bhardwaj, R., Sundramoorthy, A.K., *et al.* (2024) Advancements in Thermoelectric Materials for Efficient Waste Heat Recovery and Renewable Energy Generation. *Hybrid Advances*, **5**, Article ID: 100176. https://doi.org/10.1016/j.hybadv.2024.100176

[2] Jouhara, H., Żabnieńska-Góra, A., Khordehgah, N., Doraghi, Q., Ahmad, L., Norman, L., *et al.* (2021) Thermoelectric Generator (TEG) Technologies and Applications. *International Journal of Thermofluids*, **9**, Article ID: 100063. https://doi.org/10.1016/j.ijft.2021.100063

[3] Zhang, X. and Zhao, L. (2015) Thermoelectric Materials: Energy Conversion between Heat and Electricity. *Journal of Materiomics*, **1**, 92-105. https://doi.org/10.1016/j.jmat.2015.01.001

[4] Hona, R.K., Dhaliwal, G.S. and Thapa, R. (2022) Investigation of Grain, Grain Boundary, and Interface Contributions on the Impedance of Ca_2FeO_5. *Applied Sciences*, **12**, Article 2930. https://doi.org/10.3390/app12062930

[5] Hona, R.K., Huq, A., Mulmi, S. and Ramezanipour, F. (2017) Transformation of Structure, Electrical Conductivity, and Magnetism in AA'$Fe_2O_{6-\delta}$, A = Sr, Ca and A' = Sr. *Inorganic Chemistry*, **56**, 9716-9724. https://doi.org/10.1021/acs.inorgchem.7b01228

[6] Asenath-Smith, E., Lokuhewa, I.N., Misture, S.T. and Edwards, D.D. (2010) P-Type Thermoelectric Properties of the Oxygen-Deficient Perovskite $Ca_2Fe_2O_5$ in the Brownmillerite Structure. *Journal of Solid State Chemistry*, **183**, 1670-1677. https://doi.org/10.1016/j.jssc.2010.05.016

[7] Wang, H., Su, W., Liu, J. and Wang, C. (2016) Recent Development of N-Type Perovskite Thermoelectrics. *Journal of Materiomics*, **2**, 225-236. https://doi.org/10.1016/j.jmat.2016.06.005

[8] Shi, X., Wu, H., Liu, Q., Zhou, W., Lu, S., Shao, Z., *et al.* (2020) $SrTiO_3$-Based Thermoelectrics: Progress and Challenges. *Nano Energy*, **78**, Article ID: 105195. https://doi.org/10.1016/j.nanoen.2020.105195

[9] Jiamprasertboon, A., Okamoto, Y., Hiroi, Z. and Siritanon, T. (2014) Thermoelectric Properties of Sr and Mg Double-Substituted $LaCoO_3$ at Room Temperature. *Ceramics International*, **40**, 12729-12735. https://doi.org/10.1016/j.ceramint.2014.04.123

[10] Terasaki, I., Sasago, Y. and Uchinokura, K. (1997) Large Thermoelectric Power in $NaCo_2O_4$ Single Crystals. *Physical Review B*, **56**, R12685-R12687. https://doi.org/10.1103/physrevb.56.r12685

[11] Molinari, M., Tompsett, D.A., Parker, S.C., Azough, F. and Freer, R. (2014) Structural, Electronic and Thermoelectric Behaviour of $CaMnO_3$ and $CaMnO_{(3-\delta)}$. *Journal of Materials Chemistry A*, **2**, 14109-14117. https://doi.org/10.1039/c4ta01514b

[12] Kumar, P., Kashyap, S.C., Sharma, V.K. and Gupta, H.C. (2015) Improved Thermoelectric Property of Cation-Substituted $CaMnO_3$. *Chinese Physics B*, **24**, Article ID: 098101. https://doi.org/10.1088/1674-1056/24/9/098101